第 17 卷 第 2 期 光 学 学 报 Vol. 17, No. 2
1997 年 2 月 ACTA OPTICA SINICA February, 1997

An All-Fiber Fused Biconical Filter with Two Ring-Three Fiber Mutually Couplings

Yan Fang Chen Zhenyi Song Yuezhu
(*Communication Institute, Shanghai University, Shanghai* 201800)

Abstract In this paper, a spectral characteristic of two ring-three fiber mutually coupling filter has quantitatively analysed by assuming a total-amplitude coupling coefficient in the weakly and strongly coupling sections of the fused biconical structure to be equal to the amplitude coupling coefficient in the filtering network equations. The measured passband profile of the experimental filter is basically in agreement with the theoretical one. The measured center wavelength, regrction, half-power bandwidth and insertion loss of the investigated filter are 1.27 μm, > 13 dB, 72 μm and 3.9 dB, respectively.

Key words all-fiber, filter, fused biconical taper.

1 Introduction

As an important device, it is predicted that all-fiber filters will be widely used in optical fiber communication, sensing, lasing, information conversing, processing and spectrum analysing systems, etc. Some papers on modelling of all-fiber filters have been reported[1~9], in which network theories are normally adopted. In the theories, an amplitude coupling coefficient is introduced to deseribe the coupling process of the filtering network, but the coefficient itself is not relevant to the concretely coupling structure of the fused biconical filters. The theories, therefore, are qualitative. By our judgement, a quantitative theory on modelling of the filters has not been reported yet, which is quite important to the filter design. In this paper, the authors will introduce a mathematical model on quantitatively computing the spectral characteristic of the filters. In the light of the model, a variety of spectral characteristics of the filters can be estimated in advance. Generally speaking, the fused coupling structure is normally separated into weakly and strongly coupling sections, the formaer can be descibed by the cross coupling between the two weak-guide waveguides[18], and the laster can be explained by the interference between the two surface waves in the same dielectric waveguide[12]. Nevertheless. it is very difficult that how to define the interface of the two

Received 22 November 1995; revised 12 March 1996

kinds of coupling. The interfaces defined by different authors[10~14] can not be suitable for our situation though their definitions suit for calculation of the couplers and WDMs. It is not successful when we adopt the definitions in calculating the fused filters. In this paper, we set up a new definition for the interface where the coupling coefficient per unit length in the weakly coupling section reaches maximum and, meanwhile, the difference of the coupling coefficients per unit length between the weakly and strongly coupling sections is minimum, which means an optimum transition from the weakly coupling section to the strongly coupling section and vice versa. Based upon the new definition, the result of the theoretical calculation for the filter can basically consist with that of experiment, as shown later. In the model, the equivalence-coupling coefficient concept in the weakly and strongly coupling sections, the over-coupling concept in the filtering network and the core-core contracting ratio in the drawing process are introduced.

2 Theory

1) The configuration of the investigated filter is shown in Fig. 1. Based on the network theory[15], the network equations can be summarized below:

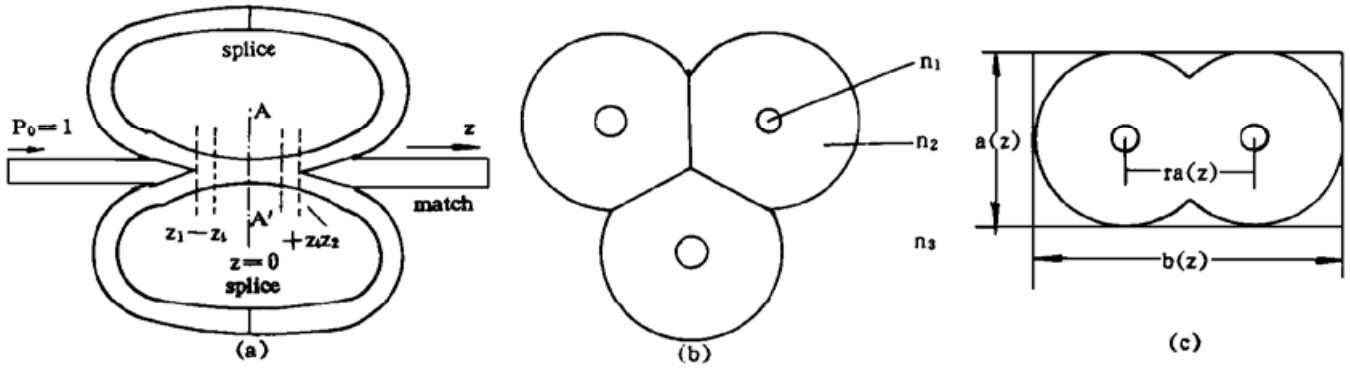

Fig. 1 (a) The configuration of the investigated filter. $z_1 - z_2$ is coupling region, (b) the triangularly coupling cross-section in the middle of the taper. (c) an equlvalence-rectangle dielectric waveguide in the strongly coupling section, r is the core-core contracting ratio in the drawing process

$$B_{i1} = \left(\sqrt{1-2k^2} + jk\sum_{i\neq i}\right)A_{i2}, \qquad B_{i2} = \left(\sqrt{1-2k^2} + jk\sum_{i\neq i}\right)A_{i1}, \qquad i = 1, 2, 3 \tag{1}$$

here, $A_{i1,2}$, $B_{i1,2}$ are scattering matrix elements, k is amplitude-coupling coefficient between arbitrary two fibers in the coupling structure, j is complex unit and shows couping wave is ahead of $\pi/2$ to throughput wave, first subscript i indicates ith fiber., second subcripts 1, 2 indicate input-port reference area z_1 and output-port reference area z_2, respectively. On the two reference areas, the boundary conditions hold:

$$A_{11} = 1, \qquad A_{12} = 0, \qquad A_{i1} = B_{i2}\exp[-(a + i\varphi)],$$
$$A_{i2} = B_{i1}\exp[-(a + j\varphi)], \qquad a = a_1 + a_2, \qquad \varphi = 2\pi n_1 l/\lambda, \qquad i \neq 1 \tag{2}$$

here, λ is operating wavelength, l is the length of the fiber ring, α is total loss, a_1 is the splicing loss of the fiber rings, a_2 is the loss in the coupling structure, n_1 is refrective index of the core of the fiber.

It is worth notice that the coupling coefficient k in equations (1) has a following form:

$$k = k[a(z), \lambda, n_i], \qquad i = 1, 2, 3 \tag{3}$$

here, n_i are the refractive indexes defined in Fig. 1, $a(z)$ is cladding diameter of an arbitrary

fiber in the fused biconical region, z is along the tapering direction. Fig. 2 shows the measured and the simulating curves of the tapering dimension. The simulating formula is listed as follows:

$$a(z) = a_0 + a_1 z + a_2 z^2 + a_3 z^3 + a_4 z^4 \qquad (4)$$

here, $a_0 = 19.4$, $a_1 = 5.3889\text{E}-3$, $a_2 = -3.1667\text{E}-6$, $a_3 = 2.3457\text{E}-9$, $a_4 = -2.5185\text{E}-13$. It has been confirmed that the measured curve satisfies adiabatic condition[16, 17]

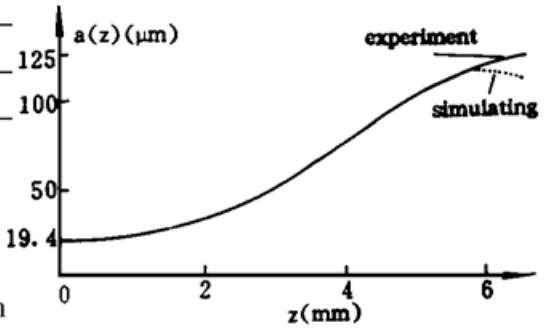

Fig. 2 The measured and simulating curves of the tapering dimension along z direction of Fig. 1 (a). The solid line is belong to experiment and the dashed line simulating

2) In the weakly coupling section, the coupling coefficient per unit length in the weak-guide waveguides can be writtern as:

$$C(a, \lambda) = \frac{\lambda}{2n_1\pi} \frac{u^2 K_0(wra/\rho)}{\rho^2 V^2 K_1^2(w)} \qquad (5)$$

here, ρ is core radius of the fiber, $V = (2\pi\rho/\lambda)\sqrt{n_1^2 - n_2^2}$ is the normalzed frequency, u and w are lateral wave numbers, K_0, K_1 are modified Bessal functions of order 0 and 1, respectively. In this case, it is worth notice that u and w are functions of $a(z)$, meanwhile, in the arbitary cross section of the tapering region, V, u and w should satisfly the characxteristic equations[16] of the "local" fundamental mode[16], as mentioned in section 2, 1). Dut to $C(a)$ varying with z, the coupling coefficient in the weakly coupling section can be writtern as:

$$C_w l_w = 2\int_{z_i}^{z_l} C[a(z)]\,dz \qquad (6)$$

here, $2z_l$ denotes the tapering length, z_i is the interface defined in Introduction.

3) In the strongly coupling section, the core of the fiber is so thin that it can be neglected. The coupling sections is deseribed by an equivalence-rectangle dielectric waveguide, within which only the local fundamental and first high-order modes interfer each other to occur coupling[19]. The coupling coefficient in this section can be expressed as:

$$C_s l_s = \int_0^{z_i} [\beta_{11}(a) - \beta_{21}(a)]\,dz \qquad (7)$$

here, β_{11} and β_{21} are propagation constants of the above two modes in the dielectric waveguide, respectively.

4) Based on the conventional definition of the coupling coefficient used in couplers and WDMs, the total-amplitude coupling coefficient of the tapering region is summarized as:

$$k_t(\lambda) = \sin[C_w l_w(\lambda) + C_s l_s(\lambda)] \qquad (8)$$

Obviously, the coupling coefficient of the filtering network, k, should be equal to the above coupling coefficient:

$$k = k_t(\lambda) \qquad (9)$$

substitution of equations (2)~(9) into equation (1), the spectral characteristic of the investigated filter can be predicted. Two calculating methods have been performed. one is in-close-form solution solved from the complex equation (1), the other is based on numberical calculation. The two results are identical exactly.

3 Experiment

The experimental process is briefly summarized below. Three same-length fibers are stripped the jackets in their middle sections, then, the sections are put through a cleaning operation. Two fibers are selected to make the fiber rings by splicing their two free ands as shown in Fig. 1(a). The three cleaned fiber sections contacted each other are attached on the platform of the bidirection-extending machine, which is controlled by microcomputer and used with an oxygen-hydrogen burner controlled by electronic massflow controllers. A monitering light at 1.3 μm from a monochrometer is injected to input fiber and measured from out fiber by a x-y recorder to observe power change during drawing process of the filter. An oscillating curve is appeared on x-y recorder, from which a suitable peak is selected to stop drawing, then the spectrum of the investigated filter is scaned by the monochrometer.

The structure parameters and the experimental data of the investigated filter are listed below:

Standard Corning fiber, cut-off wavelength λ_c = 1.24, core diameter= 9 μm, cladding diameter= 125 μm, the refractive indexes of core, cladding and air are n_1 = 1.461, n_2 = 1.458 and n_3 = 1, respectively, the biconical dimension is shown in Fig. 2 or computed from equation (4), the core-core contracting ratio in the drawing process, r = 0.6, splicing loss of the fiber rings a_1 = 0.9 dB (Adopted from the average splicing loss of the fiber splicing machine used), loss of the coupling region $a_2 = \alpha - \alpha_1$ = 3.0 dB (α is the total measured loss), the length of each fiber ring $l \doteq$ 80 cm.

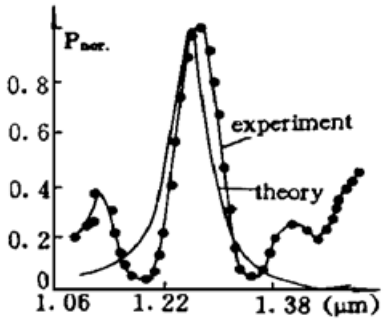

Fig. 3 The passband-spectrum curve of the investigated filter: – theory, * * experiment

The measured center wavelength, rejection (maximum power/minimum power whithin band), half-power bandwidth and insertion loss of the investigated filter are 1.27 μm, > 13 dBm 72 μm and 3.9 dB, respectively, as shown in Fig. 3. The passband-spectrum curve of the filter has been plotted. Thus, a coincidence between theoretical calculation and experiment can be seen. It is noticed that in Fig. 3, insertion less 3.9 dB has been deducted from the theoretical and the experimental curves.

Discussion In Fig. 3 the outband-side lobes are appeared in the measured curve. The reason why they occur is still unclear. The following reasons are conjectured.

1) The length of two fiber rings is not exactly identical due to measuring error and contraction at splicing point.

2) The secondarily coupling effect in the network equations is not considered.

We have not done the computation considering the above factors, because it is quite complicated.

Reference

[1] A. Safaai-Tazi, J. C. McKeeman, All-fiber spectral filters with nonperiodic bandpass characteristics and high extinction ratios in the wavelength range 0.8 μm< λ< 1.6 μm. *IEEE J. Lightwave Technol.*, 1991, **9**(8): 959~ 963

[2] M. S. Yataki, D. N. Payne, M. P. Varnham, All-fiber wavelength filters using concatenated fused-taper couplers. *Electron. Lett.*, 1985, **21**(6): 248~ 249

[3] D. Marcuse, Directional-coupler filter using dissimilar optical fibres. *Electron. Lett.*, 1985, **21**(17): 726~ 727

[4] A. C. Boucouvalas, G. Georgiou, Concatenated tapered coaxial coupler filters. *IEEE Proc. J.*, 1987, **134**(3): 191~ 195

[5] K. Okamoto, J. Noda, Fiber-optic spectral filters consisting of concatenated dual-core fibres. *Electron. Lett.*, 1986, **22**(4): 211~ 212

[6] F. Sanchez, Matrix algebra for all-fiber optical resonators. *IEEE J. Lightwave Technol.*, 1991, **9**(7): 838~ 844

[7] J. E. Bowers, S. A. Newton, M. V. Sorin *et al.*, Filter response of single-mode fiber recirculating delay lines. *Electron. Lett.*, 1982, **18**(3): 110~ 111

[8] Y. H. Ja, Optical fiber filter comprising a single-coupler fiber ring (or loop) and a double-coupler fiber mirror. *IEEE J. Lightwave Technol.*, 1991, **9**(8): 964~ 974

[9] Y. H. Ja, A single-mode optical fiber ring resonator using a plannar 3×3 fiber coupler and a sagnac loop. *IEEE J. Lightwave Technolo.*, 1994, **12**(8): 1348~ 1354

[10] F. P. Payne, C. D. Hussey, M. S. Yataki, Modelling fused single-mode-fibre couplers. *Electron. Lett.*, 1985, **21**(11): 461~ 462

[11] K. O. Hill, D. C. Johnson, R. G. Lamont, Wavelength dependence in fused biconical taper splitters; measurement and control. *IOOC-ECOC '85, Technical Digest*, Venice, Italy, 1~ 4 OCt. 1985, **1**: 567~ 570

[12] Eisenmann, Michael, Edgar Weidel, Single-mode fused biconical couplers for wavelength division miliplexing with channel spacing between 100 and 300 nm. *IEEE J. Lightwave & Technol.*, 1988, **6**(1): 113~ 119

[13] A. W. Snyder, Radiation losses due to variations of radius on dielectric or optical fibers. *IEEE Trans. Microwave Theory Tech. (USA)*, 1970, **MTT-18**(9): 608~ 615

[14] D. Marcuse, Mode conversion in optical fibers with monotonically increasing core radius. *IEEE J. Lightwave Technol.*, 1987, **LT-5**(1): 125~ 133

[15] J. L. Altman, *Microwave Circuits*, Princeton, D. Van Nostrand Company, INC., 1964: 205~ 212

[16] S. Lacroix, R. Bourbonnais, F. Gonthier *et al.*, Tapered monomode optical fibers: understanding large power transfer. *Appl. Opt.*, 1986, **25**(23): 4421~ 4425

[17] A. W. Snyder, *Optical Waveguide Theory*. London, Chapman and Hall Ltd, 1983: 410

[18] R. Vanclooster, P. Phariseau, The coupling of two parallel dielectric fibers. *I. Basic Equations*, *Physica*, 1970, **47**: 485~ 500

[19] E. A. J. Marcatili, Dielectric rectangular waveguide and directional coupler for integrated optics. *Bull. Soc. Tech. J.*, 1969, **48**(9): 2071~ 2102

双环、三纤互耦全光纤熔锥滤波器

严　方　陈振宜　宋月珠

(上海大学通讯学院通讯研究所, 上海 201800)

(收稿日期: 1995 年 11 月 22 日; 收到修改稿日期: 1996 年 3 月 12 日)

摘　要　通过将熔锥结构中强、弱耦合段的总幅度耦合系数与滤波网络方程中的幅度耦合系数等效的方法, 定量分析了双环、三纤互耦滤波器的频谱特性。实验滤波器通带特性的测试结果与理论分析基本吻合。所测滤波器的中心波长、抑制度、半功率带宽及插入损耗分别为 1.27 μm, > 13 dB、72 μm 及 3.9 dB。

关键词　全光纤,　滤波器,　熔锥。